J Solid State Electrochem (2008) 12:1017–1020
DOI 10.1007/s10008-007-0480-4

ORIGINAL PAPER

Effects of heteroatoms on doped $LiFePO_4$/C composites

H. Liu · C. Li · Q. Cao · Y. P. Wu · R. Holze

Received: 15 August 2007 / Revised: 25 October 2007 / Accepted: 19 November 2007 / Published online: 18 December 2007

Abstract A series of supervalent cation doped $Li_{1-x}M_{0.01}Fe_{0.99}PO_4$/C composites (M=Ti, Zr, V, Nb, and W) were synthesized by solid-state reaction. The effects of the heteroatoms were studied by X-ray diffraction, cyclic voltammetry, and electrochemical impedance measurement. After doping, the lattice structure of $LiFePO_4$ is not destroyed and the reversibility of lithium ion intercalation and deintercalation is improved. The diffusion coefficient of lithium ions depends on the radius of the heteroatoms. As the radius of the heteroatom is larger, the diffusion coefficient increases.

Keywords Lithium ion battery · Cathode · $LiFePO_4$ · Doping · Supervalent cation

Introduction

Presently, lithium ion batteries as widely used as advanced power sources for portable electronic applications are mostly based on $LiCoO_2$ cathode and carbon anode materials. Because of cost and toxicity of $LiCoO_2$ [1], many alternative materials were investigated to substitute the current cathode materials. Layered $LiNiO_2$ [2–4] and spinel $LiMn_2O_4$ [5–8] have been identified as positive electrode materials for high power applications. The olivine-structured $LiFePO_4$ was examined as cathode materials in 1997 [9, 10], and it was considered as the most likely promising substitute for $LiCoO_2$ because of its high operating voltage (about 3.5 V vs. Li^+/Li) attributed to the Fe^{3+}/Fe^{2+} redox couple, large theoretical capacity (170 mAh/g), good stability of the phosphate when in contact with common organic electrolytes, low cost, and environmental benignancy [11, 12].

One of the key drawbacks of $LiFePO_4$ is its low intrinsic electronic conductivity. Various synthesis and processing approaches have been employed to overcome this problem. Initially, additives were introduced to synthesize $LiFePO_4$/conductive material composites, such as dispersed carbon [13–17], metal powders [18, 19], and intrinsically conducting polymers [20]. However, only the bulk conductivity improved, not the intrinsic one of the $LiFePO_4$ lattice. Another method is doping where Li ions (on the M1 site) and/or Fe ions (on the M2 site) are substituted. It was reported that low-level doping of $LiFePO_4$ by a range of supervalent ions (e.g., Mg^{2+}, Al^{3+}, Ti^{4+}, Zr^{4+}, Nb^{5+}) increases the electronic conductivity to values greater than 10^{-2} S/cm at room temperature [21]. Besides, investigations of doping of other heteroatoms indicate that the electrochemical properties of $LiFePO_4$ could be improved by the modification [22–24].

However, to our knowledge, details of the effects of doping have not been reported. We recently reported that the electrochemical properties of $LiFePO_4$/C composite were improved by Zn doping and the doping effects were fully explored [25]. In the present study reported here, we

Contribution to ICMAT 2007, Symposium K: Nanostructured and bulk materials for electrochemical power sources, July 1–6, 2007, Singapore

H. Liu · C. Li · Q. Cao · Y. P. Wu (✉)
Shanghai Key Laboratory of Molecular Catalysis and Innovative Materials, Department of Chemistry, Fudan University,
Shanghai 200433, China
e-mail: wuyp@fudan.edu.cn

R. Holze
Institut für Chemie, AG Elektrochemie,
Technische Universität Chemnitz,
09111 Chemnitz, Germany
e-mail: rudolf.holze@chemie.tu-chemnitz.de

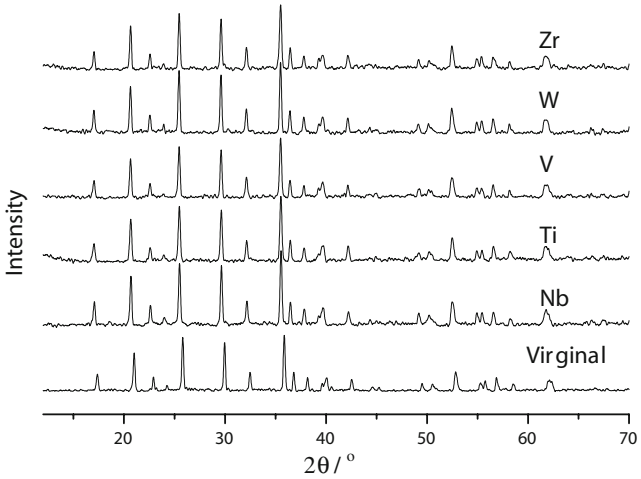

Fig. 1 X-ray diffraction patterns of the virginal and the doped $LiFePO_4/C$

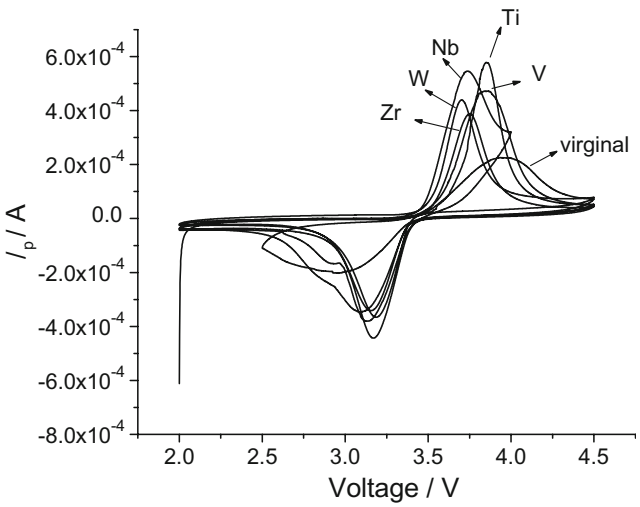

Fig. 2 CV profiles of the virginal and the doped $LiFePO_4/C$ at the scanning rate 0.5 mV/s

synthesized a series of doped $Li_{1-x}M_{0.01}Fe_{0.99}PO_4/C$ materials (M=Ti, Zr, V, Nb, W), and their doping effects were investigated for the first time.

Experimental

Virginal and 1% doped $Li_{1-x}M_{0.01}Fe_{0.99}PO_4/C$ composites (M=Ti, Zr, V, Nb, and W) samples were prepared by a solid-state route. The starting material Li_2CO_3, $FeC_2O_4{\cdot}2H_2O$, $NH_4H_2PO_4$, metal oxide (TiO_2, ZrO_2, V_2O_5, Nb_2O_5, WO_3), and 5 wt.% acetylene black were mixed in atomic ratio of Li:(Fe+M):PO_4=1:(0.99+0.01):1, and the mixtures were milled in inert atmosphere to avoid the oxidation of Fe^{2+} to Fe^{3+} in a planet mixer (QM-BP) for 24 h. After milling, the mixtures were calcined in a tube furnace at 400 °C for 10 h in an inert atmosphere to decompose oxalate and phosphate. Finally, the precursors were ground again and sintered at 750 °C for 15 h in an inert atmosphere.

Cathodes were prepared by mixing 90 wt.% active material, 5 wt.% acetylene black, and 5 wt.% polyvinylidene fluoride binder in *N*-methylpyrrolidone solvent to form a homogeneous slurry. The mixtures were coated on an aluminum foil and cut to pieces. After drying under ambient condition, the pieces were further dried under vacuum oven at 120 °C for 12 h. Finally, coin-type cells were assembled in a glove box using lithium foil as the counter and reference electrode, Celgard 2400 as the separator, and LIB315 (Guotai Huarong Chemical Plant) as the electrolyte.

Powder samples were identified using a powder X-ray diffractometer with monochromatized Cu K_α radiation. Both cyclic voltammogram (CV) and electrochemical impedance measurement (EIM) were performed in a two-electrode cell at room temperature. The CV was carried out with a scan rate of 0.5 mV/s in the range of 2.0–4.5 V. In EIM, the excitation amplitude applied to the cells was 10 mV and the frequency range was between 100 kHz and 10 mHz.

Table 1 The lattice parameters of the virginal and doped materials $LiFePO_4/C$ from XRD data

Sample	Space group	a/Å	b/Å	c/Å	Volume of unit/Å^3
$LiFePO_4$	P_{nmb}	5.9606	10.2043	4.7192	287.04
$LiNb_{0.01}Fe_{0.99}PO_4$	P_{nmb}	6.0227	10.3805	4.7201	295.09
$LiTi_{0.01}Fe_{0.99}PO_4$	P_{nmb}	6.0227	10.4059	4.7136	295.41
$LiV_{0.01}Fe_{0.99}PO_4$	P_{nmb}	6.0282	10.3974	4.7160	295.59
$LiW_{0.01}Fe_{0.99}PO_4$	P_{nmb}	6.0310	10.4101	4.7324	297.12
$LiZr_{0.01}Fe_{0.99}PO_4$	P_{nmb}	6.0282	10.4059	4.7119	295.57

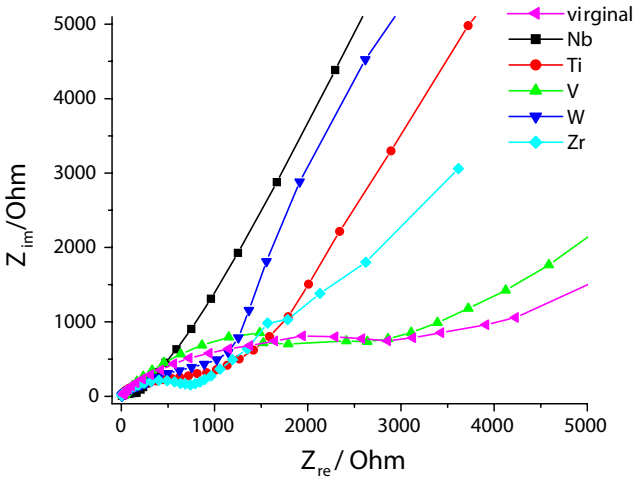

Fig. 3 The Nyquist plots of the virginal and the doped $LiFePO_4/C$ in the frequency range between 100 Hz and 10 mHz

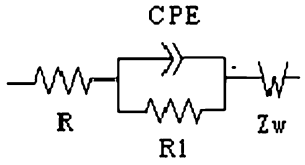

Fig. 4 The equivalent circuit of the electrode system

Result and discussion

The X-ray diffraction (XRD) patterns of virginal and doped $LiFePO_4$/C materials are shown in Fig. 1. All patterns are in good agreement with standard $LiFePO_4$ with an ordered olivine structure indexed as orthorhombic P_{nmb}. No impurity phase has been detected, which indicates that the 1% doping could not destroy the lattice structure.

It is recognized that the structure of material is crucial for its properties. The lattice parameters of materials can be calculated according to the Bragg equation from the XRD data. The quantitative results are summarized in Table 1. They indicate that doping could enlarge the volume of the crystal lattice. According to the lattice parameters, the values of *c* are less affected than those of *a* and *b*. It is reported that the lithium ion intercalation–deintercalation proceeds through one-dimensional pathways along the *c*-axis [26]. The enlarged lattice volume, namely the enlarged *a*–*b* plane, provides more space for the transfer of lithium ions, which could promote the performance of the electrode at high current density. The lattice extension is mainly attributed to the doping heteroatoms.

Cyclic voltammograms of the virginal and doped $LiFePO_4$/C are shown in Fig. 2. It is well known that the potential separation between anodic and cathodic peaks is an important parameter to evaluate the reversibility of electrochemical reactions. The cathodic–anodic peaks of the virginal material are located at 3.99/2.97 V. The separation of peaks (ΔV) is 1.02 V, which indicates high polarization during the redox process. In contrast, all ΔV values of the doped materials are decreased. For instance, the narrowest ΔV (W-doped) is 0.50 V and the widest one (V-doped) is 0.75 V. The well-defined peaks and the smaller values of potential peak separation show that the reversibility of the electrode reaction is greatly increased due to lower potential, which is consistent with the reported doping of heteroatoms [21].

The details of lithium ion migration dynamics were investigated by impedance method. Typical Nyquist plots of the doped and the virginal $LiFePO_4$ electrodes are shown in Fig. 3. All plots exhibit a semicircle in the high-frequency region and a line in the low-frequency region. The impedance data fit the equivalent circuit as shown in Fig. 4. The constant phase angle element is commonly used to describe the depressed semicircle that results from a porous electrode [27, 28]. The depressed semicircles in the high frequency region are attributed to the charge transfer process. The decreased diameters of the semicircles indicate the reduction of charge transfer resistance (R_{ct}). The linear plots in the low-frequency region are ascribed to typical Warburg behavior, which is attributed to the diffusion of lithium ions in the cathode material. The lithium ion diffusion coefficient could be calculated from the low-frequency plots according to the following equation:

$$D = R^2T^2/2A^2n^4F^4C^2\sigma^2 \quad (1)$$

where R is the gas constant, T is the absolute temperature, A is the surface area of the cathode, n is the number of electrons per molecule during oxidation, F is the Faraday constant, C is the concentration of lithium ion, σ is the Warburg factor which is relative with Z_{re}.

$$Z_{re} = R_D + R_L + \sigma\omega^{-1/2} \quad (2)$$

The relationship between Z_{re} and reciprocal square root of the angular frequency ($\omega^{-1/2}$) in the low-frequency region is shown in Fig. 5. The diffusion coefficients of lithium ions in the virginal and the doped $LiFePO_4$/C materials were calculated and summarized in Table 2.

The diffusion coefficient of the doped materials depends on the radius of doping cations, which are also listed in Table 2 [29]. It is well known that the radius of both cations and anions are based on various factors such as coordination number, electronic spin, covalent repulsive force, and polyhedral distortion. In the $LiFePO_4$ lattice, ferrous ions occupying shared corner octahedral positions [9], thus the coordination numbers of Fe^{3+}/Fe^{2+} and doping cations are six. In previous reports, it was confirmed that both Fe^{2+} and

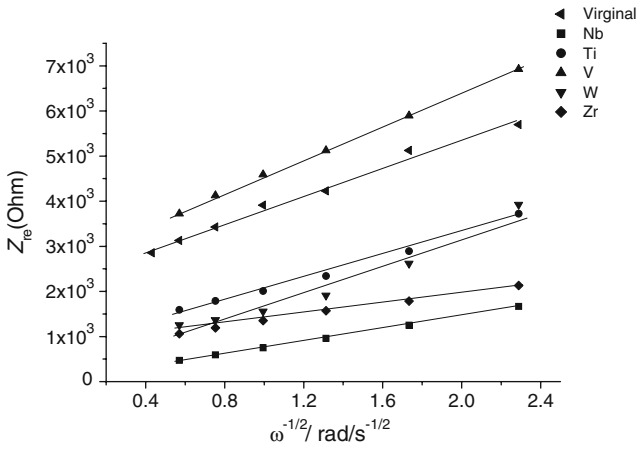

Fig. 5 The relationship between Z_{re} and $\omega^{1/2}$ at low frequency

Table 2 The calculated diffusion coefficients of lithium ions based on EIM and the radius of the doping ions

Heteroatom	Atomic radius/nm	$D_{Li}^{+}/cm^2/s$
Virginal	0.092 (Fe^{2+} HS), 0.0785(Fe^{3+} HS)	9.98×10^{-14}
V^{5+}	0.068	6.93×10^{-14}
W^{6+}	0.074	9.90×10^{-14}
Ti^{4+}	0.0745	7.78×10^{-14}
Nb^{5+}	0.078	4.90×10^{-13}
Zr^{4+}	0.086	6.18×10^{-13}

Fe^{3+} are in the high-spin (HS) state of electronic configuration [28]. After analyzing the relationship between diffusion coefficient and radius of the doping cations, as shown in Table 2, it was concluded that larger doping cations are beneficent to improve the lithium diffusion of the electrode materials. This improvement is mainly due to the pillar effect of heteroatoms [25, 30, 31]. In the case of electrochemical impedance measurement (EIM), the intercalation/deintercalation processes occur at the surface of the electrode because of alternating current applied. During charging, Fe^{2+} is changed to Fe^{3+}, causing the lattice to shrink. In this case, the larger cation (e.g., Zr^{4+}) provides more space for lithium diffusion, supports the lattice structure, and protects the structure from collapsing during charging. The diffusion coefficient of Zr-doped material increases to 6.18×10^{-13} cm^2/s from the virginal 9.98×10^{-14} cm^2/s. In contrast, the doping cations with smaller radius than that of Fe^{3+} are not so efficient to provide enough space. There should be some defects at the interface. So even if the radius of doping cations is as big as that of Fe^{3+} (0.0785nm), the diffusion coefficient of lithium ions in the Nb^{5+} (0.078nm) doped $LiFePO_4$ also increases. Perhaps the original valence of Nb was changed during the synthesis process, and further research is under way.

Conclusion

Small amount of heteroatom doped $Li_{1-x}M_{0.01}Fe_{0.99}PO_4/C$ composites (M=Ti, Zr, V, Nb, and W) were synthesized by solid-state reaction. The heteroatom doping enlarges the volume of the crystal lattice, alleviates the redox reversibility for the deintercalation and intercalation of lithium ions, and decreases the R_{ct} for the prepared doped materials in the charge transfer process. However, only when the radius of the doped heteroatom is bigger than or about equal to that of Fe^{3+} can the diffusion behavior be improved. These results provide valuable clues about further modification of $LiFePO_4$ as cathode materials for lithium ion batteries.

Acknowledgment Financial support from National Basic Research Program of China (973 Program No:2007CB209700) is greatly appreciated.

References

1. Nagaura T, Tozawa K (1990) Prog Batteries Sol Cells 209:9
2. Mizushima K, Jones PC, Wiseman PJ, Goodenough JB (1980) Mater Res Bull 15:783
3. Thomas M, David W, Goodenough JB (1985) Mater Res Bull 20:1137
4. Li C, Zhang HP, Fu LJ, Liu H, Wu YP, Rahm E, Holze R, Wu HQ (2006) Electrochim Acta 51:3872
5. Thackeray MM, Johnson PJ, De Picciotto LA, Bruce PG, Goodenough JB (1984) Mater Res Bull 19:179
6. Ohzuku T, Kitagawa M, Hirai T (1990) J Electrochem Soc 137:769
7. Tarascon JM, Guyomard D (1993) Electrochim Acta 38:1221
8. Fu LJ, Liu H, Wu YP, Rahm E, Holze R, Wu HQ (2005) Prog Mater Sci 50:881
9. Padhi AK, Nanjundaswamy KS, Goodenough JB (1997) J Electrochem Soc 144:1188
10. Padhi AK, Nanjundaswamy KS, Masquelier C, Okada S, Goodenough JB (1997) J Electrochem Soc 144:1609
11. MacNeil DD, Lu ZH, Chen ZH, Dahn JR (2002) J Power Sources 108:8
12. Takahashi M, Tobishima S, Takei K, Takahashi Y (2002) Solid State Ionics 148:283
13. Ravet N, Chouinard Y, Magnan JF, Besner S, Gauthier M, Armand M (2001) J Power Sources 97-98:503
14. Myung ST, Komaba S, Hirosaki N, Yashiro H, Kumagai N (2004) Electrochim Acta 49:4213
15. Zaghib K, Shim J, Guerfi A, Charest P, Striebel KA (2005) Electrochem Solid State Lett 8:A207
16. Spong AD, Vitins G, Owen JR (2005) J Electrochem Soc 152: A2376
17. Liu H, Fu LJ, Zhang HP, Gao J, Li C, Wu YP, Wu HQ (2006) Electrochem Solid-State Lett 9:A529
18. Croce F, Epifanio AD, Hassoun J, Deptula A, Olczac T, Scrosati B (2002) Electrochem Solid-State Lett 5:A47
19. Park KS, Son JT, Chung HT, Kim SJ, Lee CH, Kang KT, Kim HG (2004) Solid State Commun 129:311
20. Wang GX, Yang L, Chen Y, Wang JZ, Bewlay S, Liu HK (2005) Electrochim Acta 50:4649
21. Chung SY, Bloking JT, Chiang YM (2002) Nat Mater 1:123
22. Gouveia DX, Lemos V, de Paiva JAC, Souza Filho AG, Filho JM, Lala SM, Montoro LA, Rosolen JM (2005) Phys Rev B 72:24105
23. Abbate M, Lala SM, Montoro LA, Rosolen JM (2005) Electrochem Solid-State Lett 8:A288
24. Wang GX, Bewlay S, Needham SA, Liu HK, Liu RS, Drozd VA, Lee JF, Chen JM (2006) J Electrochem Soc 153:A25
25. Liu H, Cao Q, Fu LJ, Li C, Wu YP, Wu HQ (2006) Electrochem Commun 8:1553
26. Ouyang CY, Shi SQ, Wang ZX, Huang XJ, Chen LQ (2004) Phys Rev B 69:104303
27. Huang H, Yin SC, Nazar LF (2001) Electrochem Solid State Lett 4:A170
28. Yamada A, Chung SC, Hinokuma KJ (2001) J Electrochem Soc 148:A224
29. Shannon RD (1976) Acta Cryst A 23:751
30. Kawakita J, Makino K, Katayama Y, Miura T, Kishi T (1998) J Power Sources 75:244
31. Wu YP, Rahm E, Holze R (2002) Electrochim Acta 47:3491